

Facile synthesis of silver nanoparticles and its antibacterial activity against *Escherichia coli* and unknown bacteria on mobile phone touch surfaces/computer keyboards

T. Ranjeth Kumar Reddy¹ · Hyun-Joong Kim¹

Received: 20 January 2016 / Accepted: 6 June 2016 / Published online: 13 June 2016
© Springer-Verlag Berlin Heidelberg 2016

Abstract In recent years, there has been significant interest in the development of novel metallic nanoparticles using various top-down and bottom-up synthesis techniques. Kenaf is a huge biomass product and a potential component for industrial applications. In this work, we investigated the green synthesis of silver nanoparticles (AgNPs) by using kenaf (*Hibiscus cannabinus*) cellulose extract and sucrose, which act as stabilizing and reducing agents in solution. With this method, by changing the pH of the solution as a function of time, we studied the optical, morphological and antibacterial properties of the synthesized AgNPs. In addition, these nanoparticles were characterized by Ultraviolet–visible spectroscopy, transmission electron microscopy (TEM), field-emission scanning electron microscopy, Fourier transform infrared (FTIR) spectroscopy and energy-dispersive X-ray spectroscopy (EDX). As the pH of the solution varies, the surface plasmon resonance peak also varies. A fast rate of reaction at pH 10 compared with that at pH 5 was identified. TEM micrographs confirm that the shapes of the particles are spherical and polygonal. Furthermore, the average size of the nanoparticles synthesized at pH 5, pH 8 and pH 10 is 40.26, 28.57 and 24.57 nm, respectively. The structure of the synthesized AgNPs was identified as face-centered cubic (fcc) by XRD. The compositional analysis was determined by EDX. FTIR confirms that the kenaf cellulose extract and sucrose act as stabilizing and reducing agents for the silver

nanoparticles. Meanwhile, these AgNPs exhibited size-dependent antibacterial activity against *Escherichia coli* (*E. coli*) and two other unknown bacteria from mobile phone screens and computer keyboard surfaces.

1 Introduction

The discovery of metallic nanoparticles has led to their application in various fields, such as water treatment, medicine, catalysis, biotechnology, optoelectronics, photonics, biological tagging and ecological pollution control [1–3]. The synthesis of nanoparticles and their characterization is of tremendous interest because of potential applications in the fields of physics, biology and chemistry. At present, it is important to develop eco-friendly and sustainable techniques for producing non-toxic nanoparticles [4, 5]. Moreover, the focus of this field has shifted toward green chemistry and bioprocessing because of the utilization of eco-friendly materials, including plant leaf extracts, fruits and bacteria. These materials are inexpensive and versatile as reducing and stabilizing agents for the biosynthesis of silver nanoparticles (AgNPs). AgNPs have been of interest as next-generation antimicrobial agents because of their strong antimicrobial activity [6, 7]. There have been several biological synthesis studies on AgNPs using plant extracts, such as *Solanum nigrum* L, and plant material used for synthesizing AgNPs, and the size of AgNPs was identified as 56.6 nm with spherical to polyhedral shape. These nanoparticles imply in larvicidal bioassay, and it suggested a perfect environmentally friendly compound to regulate the mosquito larvae and some other dangerous bacteria [8]. *Trachyspermum Ammi* and *Papaver somniferum* plant extractions were used for synthesizing AgNPs, since *Trachyspermum Ammi* consists

✉ Hyun-Joong Kim
hjokim@snu.ac.kr

¹ Laboratory of Adhesion and Bio-Composites, Program in Environmental Materials Science, College of Agriculture and Life Sciences, Seoul National University, Seoul 151-921, Republic of Korea

of thymol, p-cymene and -terpene and *Papaver somniferum* consists of morphine and codeine. *Trachyspermum Ammi* plays a vital role in reducing of AgNPs and its antibacterial activity [9]. Ajitha et al. [10] investigated on *Lantana-Camera*-mediated AgNPs and evaluated the antibacterial activity on four different test pathogens; Gram- negative *Escherichia coli*, *Pseudomonas* spp., *Gram-positive Bacillus* spp. and *Staphylococcus* spp. The corresponding reports suggest the green synthesized silver nanoparticles showed great response against all tested pathogens and antibacterial activity. The diameter of zone of inhibition was higher at low size of nanoparticle and very low at high size of nanoparticle. *Terminalia chebula* fruit extract was used for synthesizing silver nanoparticles, and the size of the particle was around 25 nm with face-centered cubic geometry. It was found the synthesized AgNPs have good catalytic activity in the reduction of methylene blue [11]. Moreover, AgNPs reduced without any catalyst, template or surfactant by using *Eucalyptus oleosa*. The primary importance of this synthesis, it saves time of synthesis reaction and gets optimized AgNPs [12]. An antibacterial study was done by using nanocrystalline silver particles, which were extracted from *Cinnamon zeylanicum bark*. In this study, it was identified the pH played a vital role in size control of particles [13]. In addition, *Crataefus douglasii* [14] cyanobacteria and microalgae [15], *Azadirachta indica* [16], *Terminalia arjuna* [17] plant materials have been used for reducing and stabilizing AgNPs [18]. Although an antibacterial activity of AgNPs for different pathogenic microorganisms has been studied and elucidated the zone of inhibition increases with decreasing the size of nanoparticles, no researchers have investigated their effect on the bacteria persistent on the surface of touch-based devices.

One of the most abundant plant materials, kenaf (*Hibiscus cannabinus*), has attracted great attention over the last few years, and its cellulose fibers could serve as a raw material for the pulp and paper industry [19]. Batik manufacturing is an industry that generates a high amount of waxes in its wastewater. The kenaf core is a good absorbent for the waxes because of its characteristics [20]. There is significant interest growing worldwide for eco-friendly compatible materials and renewable resources, and this has brought about substantial scientific and technological research in the field of cellulose [21].

In this work, we focused on the green synthesis of AgNPs using the cellulose extraction of kenaf (*H. cannabinus*) biomass as a stabilizing agent and sucrose as a reducing agent, as well as the synthetic mechanism. In addition, the material's antibacterial activity for *Escherichia coli* (*E. coli*) and two other unknown bacteria present on mobile phone screens and computer keyboard surfaces was investigated. To the best of our knowledge, we are

reporting this activity using the green synthesis of AgNPs for the first time.

2 Materials and methods

Kenaf fibers were bast fibers donated by the Sutongsang Company, South Korea. Silver nitrate (AgNO_3) with $\geq 99.5\%$ purity was purchased from Sigma-Aldrich, South Korea. Sucrose, HCl, sodium chlorate and sodium hydroxide pellets were purchased from Sigma-Aldrich, South Korea. All of the analytical grade chemicals were used without additional purification.

2.1 Extraction of cellulose from kenaf fibers

The collected kenaf bast was milled into small pieces using a blender. The resulting material was treated with 4 % w/w NaOH solution at 80 °C for 2 h. This procedure was repeated four times. After this treatment, the fibers were thoroughly washed with distilled water to remove the alkali. Then, the alkali-treated fibers were bleached using identical concentrations of acetic acid and sodium chlorate (1.7 % w/w) in distilled water. This bleaching process was carried out five times at 80 °C for 2 h. Afterward, the fibers were allowed to dry at room temperature [22].

2.2 Preparation of cellulose solution

After the alkaline and bleaching treatments, the fibers were diced into fine pieces using a homogenized blender. The cellulose fiber (2 gm) was dissolved in 100 mL of distilled water and boiled at approximately 150 °C, which causes the breakdown of the polysaccharides in cellulose.

2.3 Synthesis of silver nanoparticles

One hundred milliliters of a 0.001 M aqueous solution of silver nitrate was prepared in three separate flasks. The cellulose solution, a sucrose solution (2 g of sucrose in 20 mL of distilled water) and the silver nitrate solution were combined in a ratio of 1:1:5. The original pH of the solution was 8.0, and this was adjusted to pH 5 and pH 10 by adding 0.5 M HCl and 0.25 M NaOH. These flasks were kept at 90 °C for 24 h. To monitor the reactions, we took aliquots at different reaction times.

2.4 Characterizations

The synthesized silver nanoparticles were characterized by various techniques. The absorption spectra of the synthesized AgNPs were analyzed using a Perkin–Elmer Lambda 25 UV–visible spectrometer with a range of 300–800 nm.

The size, morphology and composition of the AgNPs were determined by transmission electron microscopy (TEM). For this analysis, the samples were placed on a carbon-coated copper grid and examined using a JEOL 2100 at a working voltage of 200 kV. FE-SEM (SUPRA 55VP-31-04) operating at EHT and 2 kV and energy-dispersive X-ray spectroscopy were also used for morphological and elemental analyses. To determine the structure of the

synthesized AgNPs, a solution was placed on a microscope glass slide and allowed to dry in hot air oven at 50 °C; this process was repeated until a layer formed on the glass slide. These dried samples were analyzed by an XRD instrument (Bruker D8 ADVANCE with DAVINCI, Germany) at an operating voltage of 40 kV and a current of 40 mA with a Cu source (1.5418 Å) in film mode. The scanning region of 2θ is from 20° to 80°. For FTIR

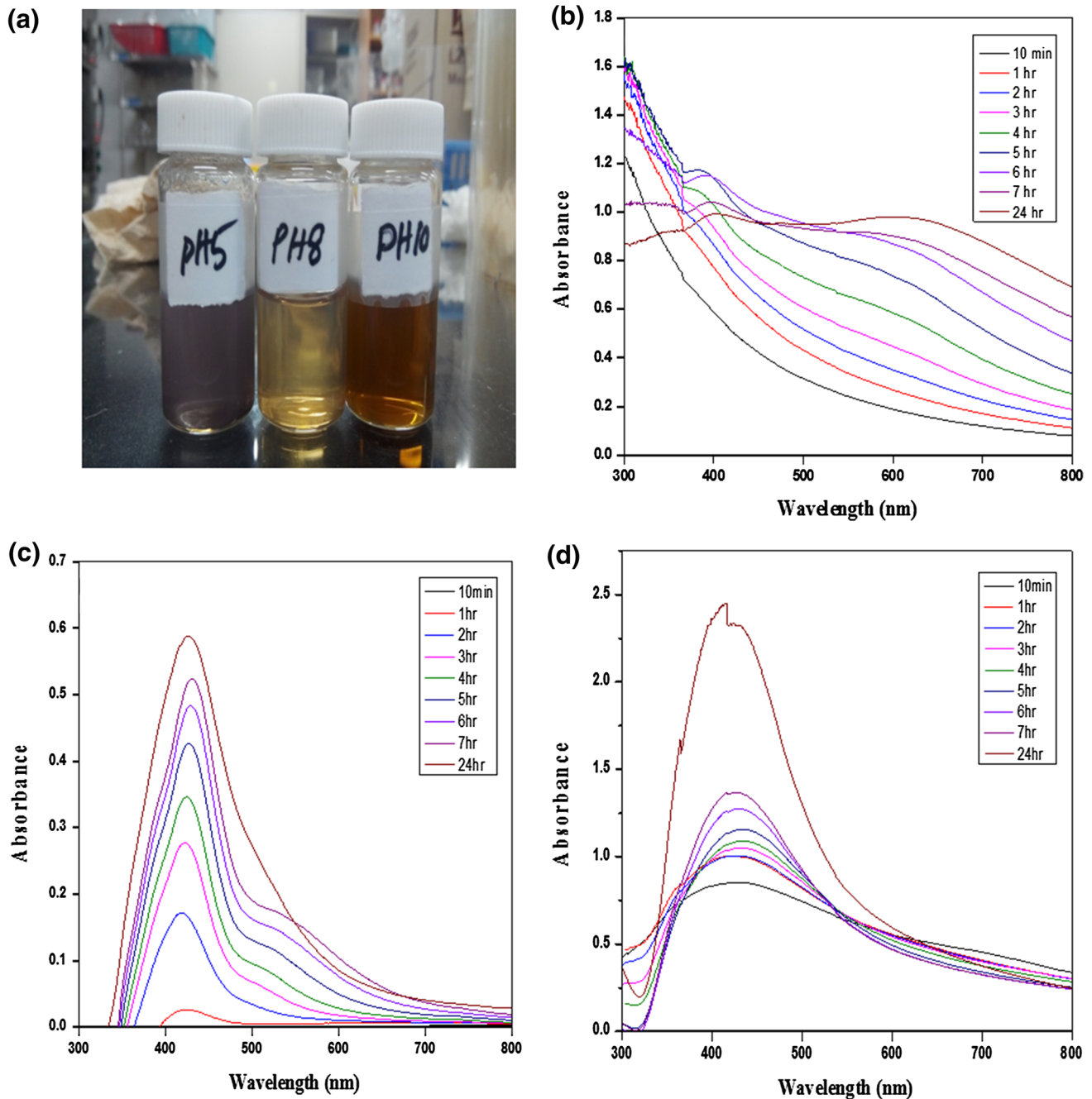


Fig. 1 a Color intensity of green synthesized AgNPs from kenaf cellulose extract with sucrose. b, c and d Color intensity of UV-Vis spectral peak of green synthesized AgNPs at pH 5, pH 8 and pH 10

analysis, the synthesized silver nanoparticle solution was centrifuged at 13,000 rpm for 15 min. The resulting solid was re-suspended in 5 mL of distilled water and lyophilized for 12 h. Fourier transform infrared spectroscopy (FTIR) (Spectrum One, Perkin–Elmer, Waltham, MA, USA) was performed from 4000 to 400 cm^{-1} with a resolution of 2 cm^{-1} and five scans per spectrum. FTIR samples were prepared from 1 mg of finely powdered silver nanoparticles and 200 mg of KBr.

2.5 Antibacterial assay

The antibacterial activity of the synthesized AgNPs was investigated using a standard disk diffusion method. The bacterial test organisms, *E. coli* and two unknowns were cultured in a nutrient broth for 24 h. The pre-prepared nutrient agar media were transferred to sterilized Petri dishes for solidification. After solidification of the media, the bacterial colonies of test organisms (50 μL) were

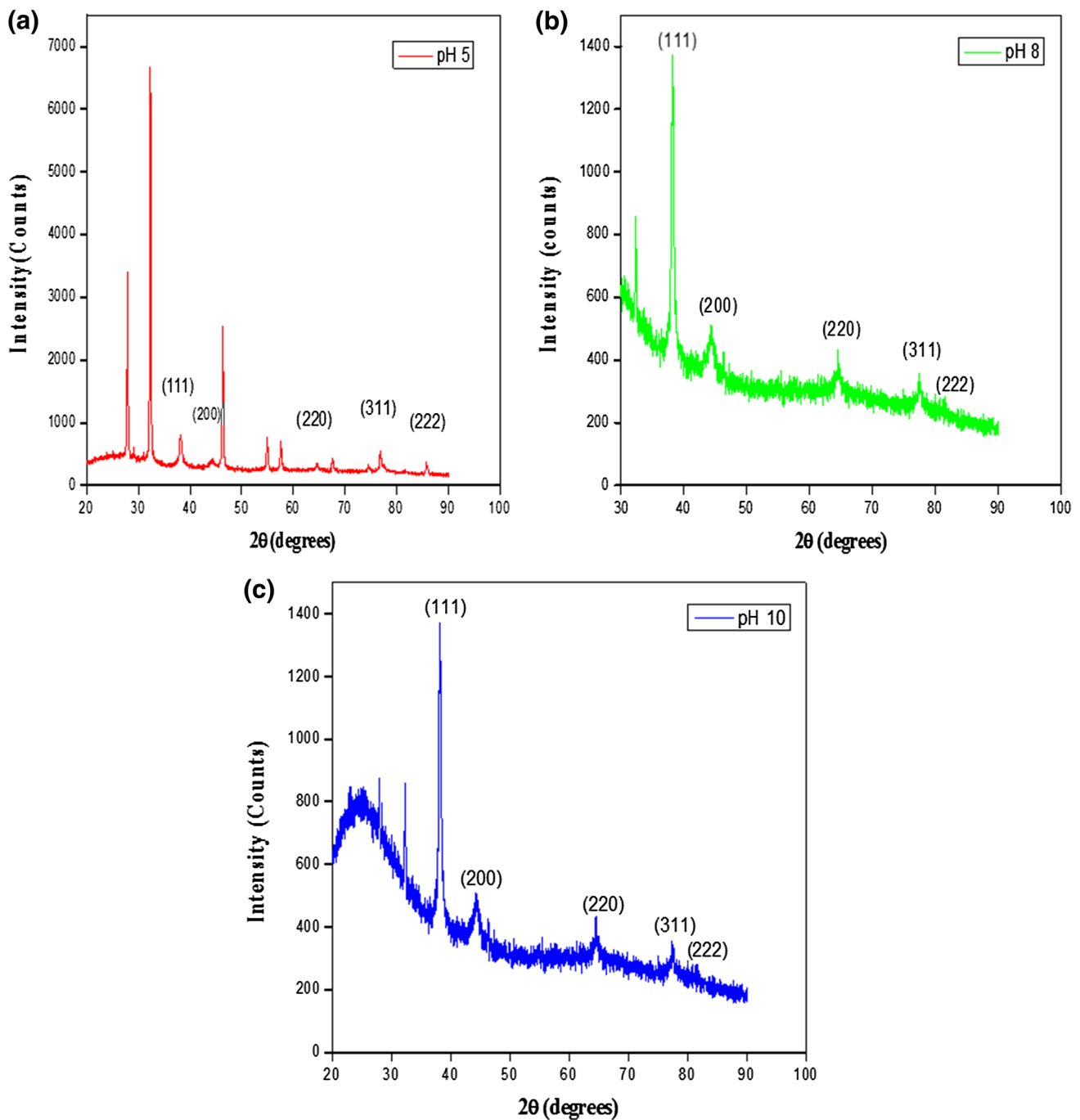


Fig. 2 XRD patterns of the AgNPs at **a** pH 5 **b** pH 8 **c** pH 10

spread on top of the nutrient agar media with a sterile bent glass rod. Then, sterilized paper disks (3 mm) were loaded with synthesized AgNPs at pH 5, pH 8 and pH 10 and placed onto the agar media. The petri dishes with AgNP disks were placed in an incubator at 37 °C for 2 days. After this period, the observed inhibition zones surrounding each disk were photographed and measured with a ruler.

3 Results and discussion

3.1 UV-visible spectroscopic analysis

In this analysis, the extracted cellulose solution from the kenaf fiber acted as a stabilizer, and the sucrose acted as a

reducing agent. At pH 10, the solution color was observed to change from white to yellow within 10 min. With time, the color changed from light yellow to brown, as shown in Fig. 1a. The reactions at pH 10, pH 8 and pH 5 were kept at 90 °C for 24 h. During this period, the color of the solution at pH 8 gradually increased with reaction time and became brown after 7 h. For the solution at pH 5, the color also gradually increased with time and became light pink, which may be an effect of the acidity. The reaction rate of the solution at pH 10 was faster than those of the solutions at pH 8 and pH 5. The UV-visible spectra are shown in Fig. 1b–d. The spectra clearly indicate that the surface plasmon resonance (SPR) increased with the rate of the reaction. A broad size distribution of small silver nanoparticles formed in the basic (pH 10) solution may be

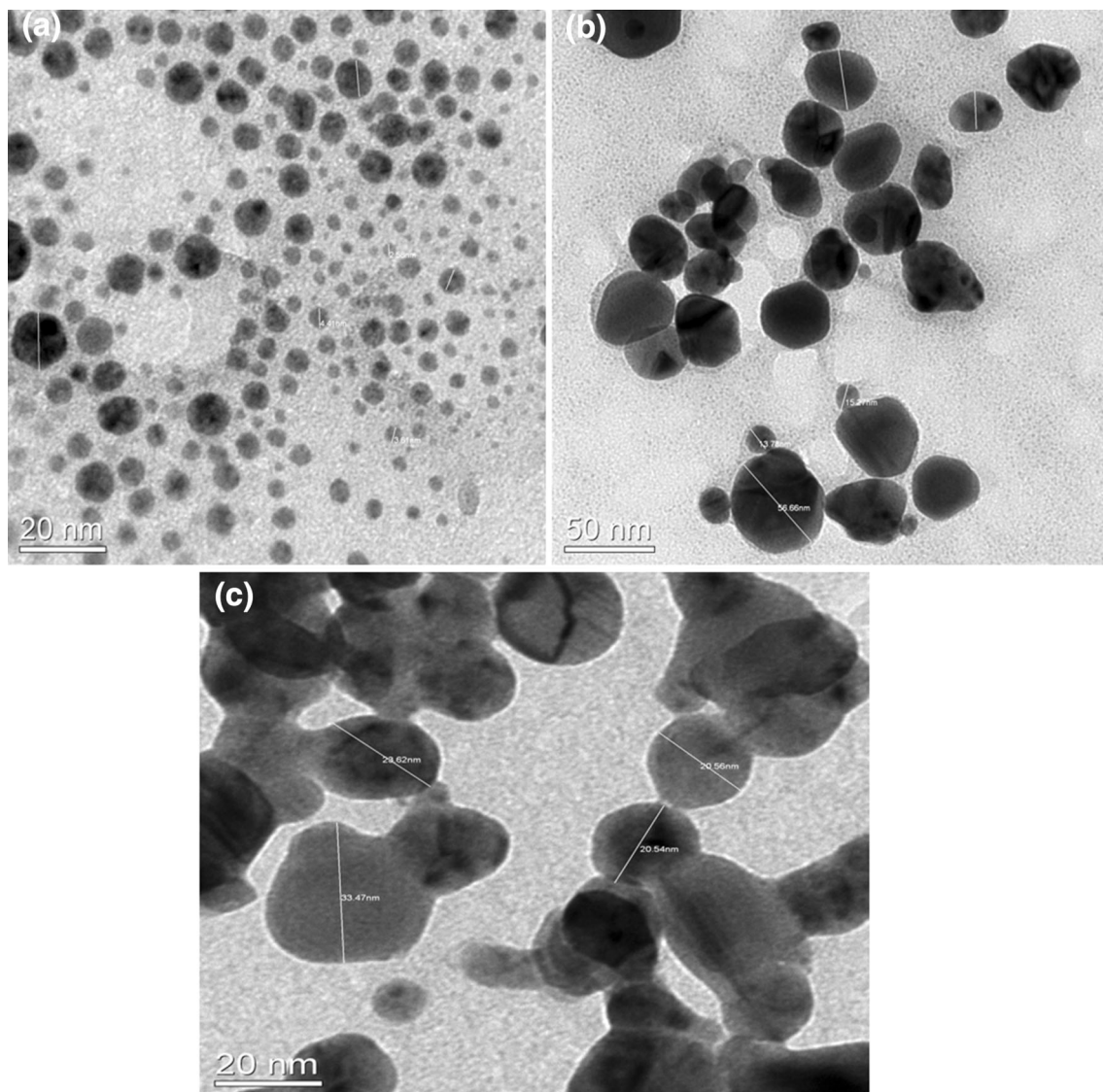


Fig. 3 TEM micrograms of the AgNPs at **a** pH 5 **b** pH 8 **c** pH 10

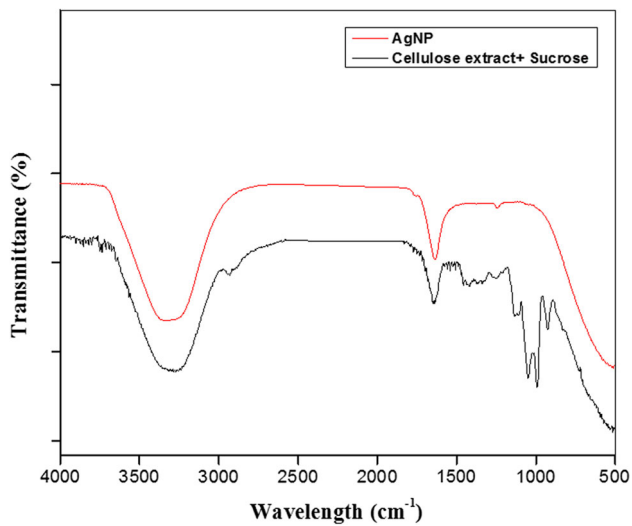


Fig. 4 FTIR image of the kenaf cellulose extract with sucrose and AgNPs

due to the existence of hydroxyl groups. No specific absorption peak was observed in the UV–visible spectra of the acidic medium (pH 5), and after 7 h, sedimentation occurred, suggesting the formation of large nanoparticles. However, at pH 8, with increasing reaction time at a constant temperature, the observed absorption peak in the desired range of 410 to 414 nm increased in intensity because of the surface plasmon resonance electrons. This result indicates that small nanoparticles formed in the basic medium, which is confirmed by the TEM analysis.

3.2 XRD analysis

The XRD patterns of the green synthesized silver nanoparticles at pH 5, pH 8 and pH 10 are shown in Fig. 2a–c. The diffraction peaks at $2\theta = 38.18^\circ$, 44.47° , 64.57° , 77.62° and 81.57° correspond to the (111), (200),

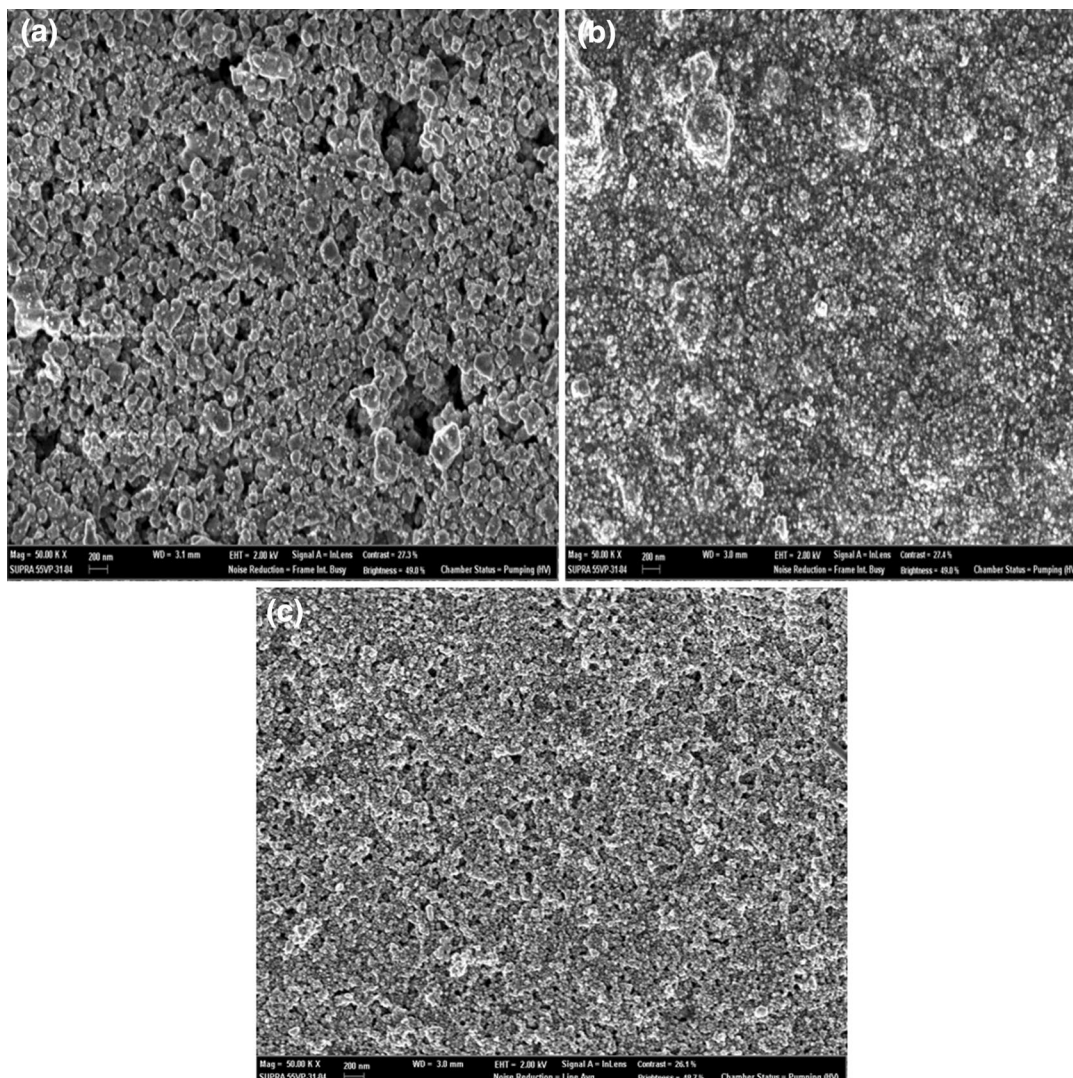


Fig. 5 FE-SEM micrographs of synthesized AgNPs at a pH 5 b pH 8 c pH 10

(220), (311) and (222) reflection planes of the face-centered cubic (fcc) structure of the silver substrate (JCPDS card, no. 87-720). The unidentified peaks are due to the presence of organic impurities. This result confirms the crystalline nature of the synthesized AgNPs [23]. The average size of the synthesized AgNPs was determined using the Debye–Scherer formula, $D = k\lambda/\beta \cos \theta$, where D is the diameter of the particle, k is a constant equal to 1, λ is

the wavelength (FWHM), and θ is the diffraction angle corresponding to the (111) lattice plane. The average crystalline grain size varied from 42 to 28 nm [24].

3.3 TEM analysis

The TEM images afford valuable information regarding the size and shape of the AgNPs. The representative TEM

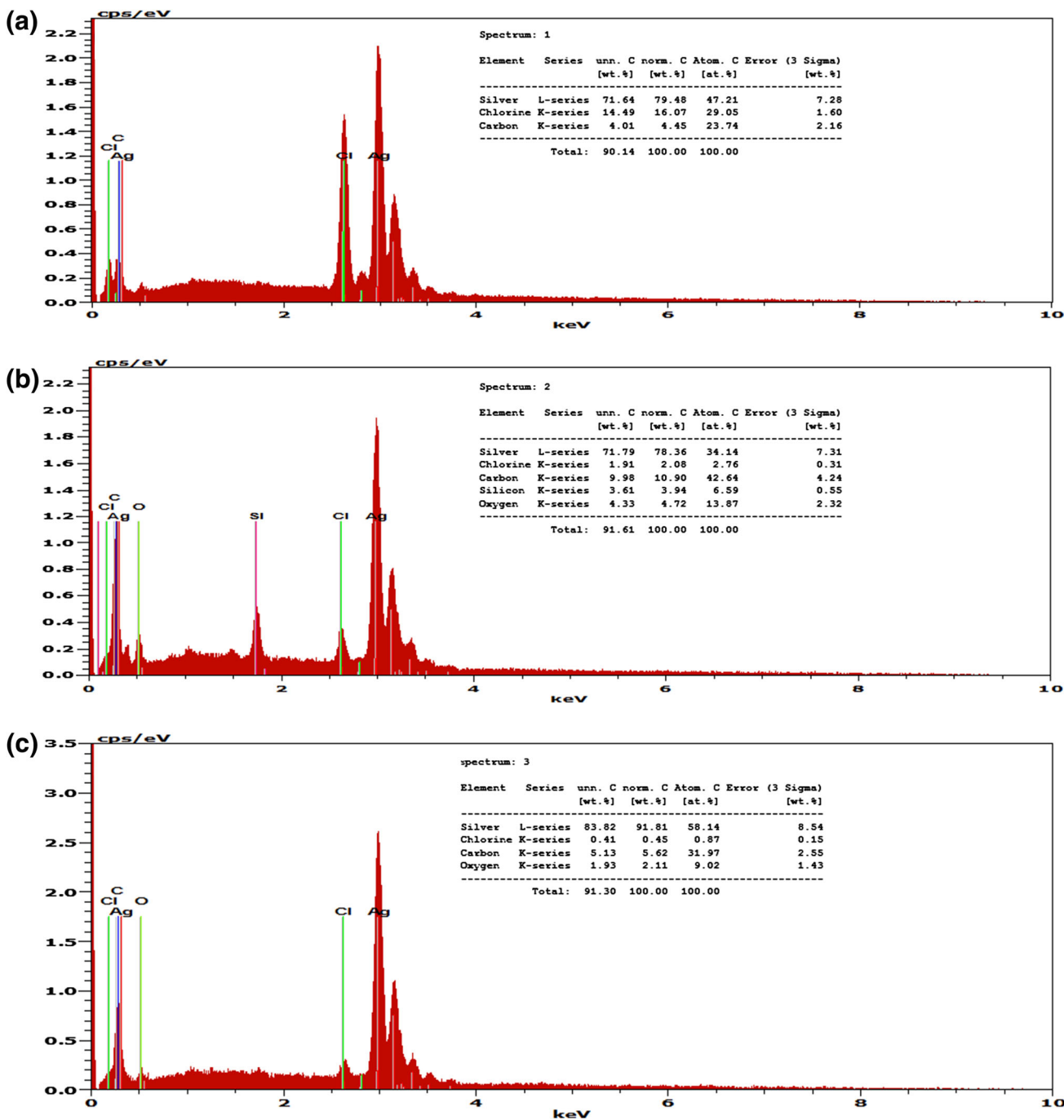


Fig. 6 EDX Spectra of synthesized AgNPs at a pH 5 b pH 8 c pH 10

images of the silver nanoparticles at different magnifications for different pH values are presented in Fig. 3a–c. From Fig. 3a–c, the average diameter of the synthesized silver nanoparticles was determined to be 40.26 nm at pH 5, 28.57 nm at pH 8 and 24.57 nm at pH 10. These values are in good agreement with XRD results. In most syntheses, spherically shaped AgNPs have been identified. However, as per the TEM micrograms, the shapes of the AgNPs synthesized here were spherical and polygonal at different pH values. That the size of the nanoparticles varies with pH is a spectacular effect; small AgNPs were observed at pH 10, while large AgNPs were obtained at pH 5. These data clearly reveal that the alkaline pH environment enhanced the reducing and stabilizing capability of the kenaf-based cellulose extract and sucrose [25].

3.4 FTIR analysis

FTIR spectroscopy is helpful to analyze the possible interactions of silver nanoparticles with different functional groups. As shown in Fig. 4, there are various functional groups at different positions in the spectrum. The strong band at 1649 cm^{-1} corresponds to bending vibration of alcoholic-OH groups. During the process of reduction of silver ions to metallic silver, the released glucose is oxidized to gluconic acid, which encapsulated to AgNPs [26]. Another intense band at 3306.6 cm^{-1} corresponds to both $-\text{NH}_2$ in primary aromatic amines and the $-\text{OH}$ groups in alcohols. The IR peaks for amide I and amide II arise owing to the carbonyl stretch and $-\text{NH}$ stretch in the amide linkage of the proteins and thereby having a greater affinity for the silver nanoparticles [10]. Similar spectra were obtained for the samples formed at pH 5 and pH 8. The alcoholic-OH groups and hydroxyl groups present in carbohydrates are influential as reducing agents, and they may be the source of the bioreduction of Ag^+ ions to Ag^0 nanoparticles during the synthesis. It was also confirmed that these alcoholic-OH groups have the strong ability to bind to metal ions, and they encapsulated the nanoparticles, forming a protective shield to prevent agglomeration. Therefore, sucrose and the cellulose extract both act as reducing and stabilizing agents in the synthesis of the nanoparticles.

3.5 FE-SEM and EDX analysis

The surface morphology of the cellulose extract and base-synthesized silver nanoparticles was studied by FE-SEM. In this analysis, we focused on the shape and

aggregation of the nanoparticles. As shown in Fig. 5a–c, the dispersed silver nanoparticles exhibited spherical and polygonal shapes at pH 5, pH 8 and pH 10, which is in good agreement with the TEM results. It was also observed that most of the nanoparticles aggregated; only a few were isolated. The elemental analysis of the synthesized silver nanoparticles was obtained with an energy-dispersive X-ray spectroscopy (EDX) accessory, as shown in Fig. 6a–c. The EDX image shows an intense silver signal and weak O, Cl, Si and C peaks, which may arise due to the presence of the biomolecules that encapsulated the surface of the AgNPs [27]. The purest silver composition was obtained at pH 10, and this result is in good agreement with the UV–visible spectroscopy study. The absorption peak of metallic silver nanoparticles generally occurs at 3 keV because of the surface plasmon resonance [28].

3.6 Antibacterial study

The antibacterial activity of green synthesized AgNPs against *E. coli* is depicted in Fig. 7a–c. The data clearly indicate an increase in the inhibition zone diameters, which depends on the pH of the solution. The greatest zone of inhibition was observed with the AgNPs synthesized at pH 10 (9 mm) compared with those synthesized at pH 5 (5 mm) and pH 8 (2 mm). As known from the TEM results, the AgNPs synthesized at pH 10 were small compared with those synthesized at pH 5 and pH 8. The

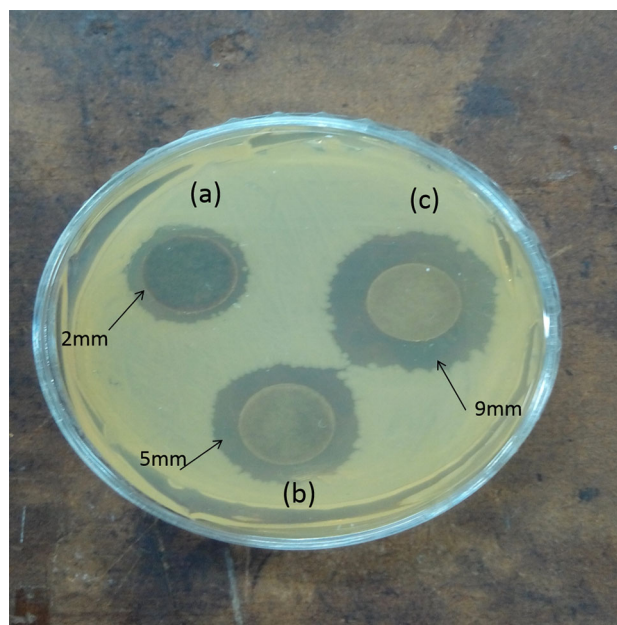


Fig. 7 Antibacterial activity against *E. coli*. of AgNPs at a pH 5 b pH 8 c pH 10

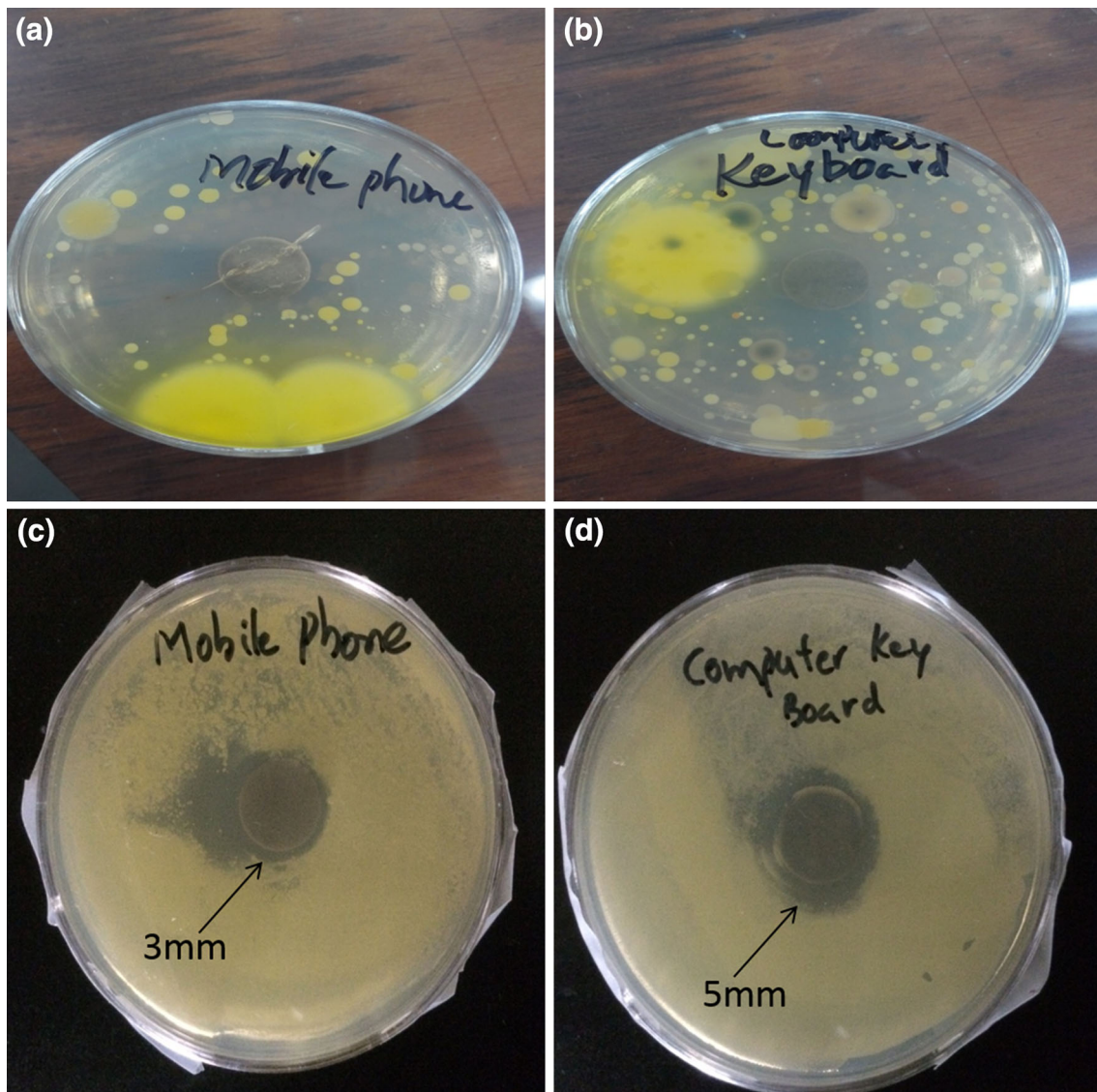


Fig. 8 Culture broth of unknown bacterial on mobile phone touch surface (a) and computer keyboard (b) and its antibacterial activity at (c) and (d)

size of the nanoparticles also influences the antibacterial activity. The smaller nanoparticles have a cumulative larger surface area, which causes the particles to interact more with bacteria than the larger particles. With the confirmation of antibacterial activity against *E. coli.*, we tested the two unknown bacteria, which are persistent on mobile phone screens and computer keyboard surfaces. Fig. 8a, b represents the overnight culture that was developed on the agar media. A spectacular effect was observed while testing with pH 10 range AgNPs, wherein the inhibition zone was observed surrounding the disk on average 3 mm and 5 mm in Fig. 8c, d. This result is in good agreement with our prediction. Overall, the green synthesized AgNPs acted perfectly as an antibacterial agent.

4 Conclusions

The green synthesis of AgNPs, using a kenaf cellulose extract solution and sucrose as stabilizing and reducing agents, respectively, is an environmentally friendly, simple and active route for the synthesis of metallic nanoparticles. These synthesized AgNPs are well dispersed, small, spherical and polygonal in shape. The particles are 40.26, 28.27 and 24.57 nm in size when synthesized at pH 5, pH 8 and pH 10, respectively. Moreover, these AgNPs worked effectively against the tested bacterial cultures. We confirmed that the unknown bacteria on mobile phone touch screens and computer keyboard surfaces accumulate with regular use without cleaning. To overcome this problem, we recommended the touch surfaces on any other

electronic devices are necessary to incorporate AgNPs for eradicating bacterial growth and transformation while using other persons. However, the more research also needed in this similar study individually on more electronic devices.

References

1. N. Barkalina, C. Charalambous, C. Jones, K. Coward, *Nanomed. Nanotech. Biol. Med.* **10**, 921–938 (2014)
2. S. Raja, V. Ramesh, V. Thivaharan, *J. Ind. Eng. Chem.* **29**, 257–264 (2015)
3. M. Ghaedi, M. Yousefinejad, M. Safarpour, H. Zare Khafri, M.K. Purkait, *J. Ind. Eng. Chem.* **31**, 167–172 (2015)
4. M. Ali, B. Kim, K. Belfield, D. Norman, M. Brennan, G.S. Ali, *Mater. Sci. Eng. C* **58**, 359–365 (2016)
5. M. Yousefzadi, Z. Rahimi, V. Ghafori, *Mater. Lett.* **137**, 1–4 (2014)
6. V. Venkatpurwar, V. Pokharkar, *Mater. Lett.* **65**, 999–1002 (2011)
7. N. Jayaprakash, J.J. Vijaya, L.J. Kennedy, K. Priadharsini, P. Palani, *Mater. Lett.* **137**, 358–361 (2014)
8. A. Rawani, A. Ghosh, G. Chandra, *Acta Trop.* **128**, 613–622 (2013)
9. K. Vijayaraghavan, S.P.K. Nalini, N.U. Prakash, D. Madhankumar, *Colloids Surf. B Bio-interfaces* **94**, 114–117 (2012)
10. B. Ajitha, Y.A.K. Reddy, P.S. Reddy, *Mater. Sci. Eng. C* **49**, 373–381 (2015)
11. T.J.I. Edison, M.G. Sethuraman, *Process. Biochem.* **47**, 1351–1357 (2012)
12. S.M. Pourmortazavi, M. Taghdiri, V. Makari, M. Rahimi-Nasrabadi, *Spectrochim. Acta A Mol. Biomol. Spectrosc.* **136**, 1249–1254 (2015)
13. X. Guangnian, Q. Xueliang, Q. Xiaolin, C. Jianguo, *Rare Met. Mater. Eng.* **42**, 0249–0253 (2013)
14. M. Ghaffari-Moghaddam, R. Hadi-Dabanlou, *J. Ind. Eng. Chem.* **20**, 739–744 (2014)
15. V. Patel, D. Berthold, P. Puranik, M. Gantar, *Biotech. Rep.* **5**, 112–119 (2015)
16. S. Ahmed, Saifullah, M. Ahmad, B.L. Swami, S. Ikram, *J. Radiat. Res. Appl. Sci.* **9**, 1–7 (2016)
17. S. Ahmed, S. Ikram, J. Nanomed. *Nanotechnol.* **6**, 309 (2015)
18. S. Ahmed, M. Ahmad, B.L. Swami, S. Ikram, *J. Adv. Res.* **7**, 17–28 (2016)
19. C.P. Neto, A. Seca, D. Fradinho, M.A. Coimbra, F. Domingues, D. Evtuguin, A. Silvestre, J.A.S. Cavaleiro, *Ind. Crops. Prod.* **5**, 189–196 (1996)
20. Y.C. Wong, S.H. Lim, N.A. Atiqah, *Pre. Environ. Sustain. Dev.* **7**, 291–295 (2013)
21. M. Haytham, M. Ibrahim, *J. Radiat. Res. Appl. Sci.* **8**, 265–275 (2015)
22. T. Mochochoko, S.O. Oluwafemi, N.D. Jumbam, P.S. Songca, *Carbohydr. Polym.* **98**, 290–294 (2013)
23. V. Ahluwalia, J. Kumar, R. Sisodia, N.A. Shakil, S. Walia, *Ind. Crops Prod.* **55**, 202–206 (2014)
24. S. Muthukrishnan, S. Bhakya, T. Senthil Kumar, M.V. Rao, *Ind. Crops. Prod.* **63**, 119–124 (2015)
25. M.M.H. Khalil, E.H. Ismail, K.Z. El-Baghdady, D. Mohamed, *Arab. J. Chem.* **7**, 1131–1139 (2014)
26. S.M. Meshram, S.R. Bonde, I.R. Gupta, A.K. Gade, M.K. Rai, *IET Nanobiotechnol.* (2013). doi:[10.1049/iet-nbt.2012.0002](https://doi.org/10.1049/iet-nbt.2012.0002)
27. B.K. Salunke, J. Shin, S.S. Sawant, B. Alkotaini, S. Lee, B.S. Kim, *Korean J. Chem. Eng.* **31**, 2035–2040 (2014)
28. M. Ramar, B. Manikandan, P.N. Marimuthu, T. Raman, A. Mahalingam, P. Subramanian, S. Karthick, A. Munusamy, *Spectrochim. Acta A Mol. Biomol. Spectrosc.* **140**, 223–228 (2015)